

# Probing quantum entanglement and collectivity effects in e+p collisions at HERA H1

Chuan Sun<sup>1\*</sup> for the H1 collaboration

1 Shandong University  
\*sunchuan@sdu.edu.cn

July 31, 2021



*Proceedings for the XXVIII International Workshop  
on Deep-Inelastic Scattering and Related Subjects,  
Stony Brook University, New York, USA, 12-16 April 2021  
doi:10.21468/SciPostPhysProc.?*

## Abstract

Charged particle multiplicity spectra are measured at HERA H1 in DIS process at  $\sqrt{s}=319$  GeV. The hadron entropy determined from the multiplicity spectra is compared to the gluon entropy predicted from a quantum-entanglement model. On the other hand, observed collective behaviours in high multiplicity  $pA$ ,  $pp$  and ultra-peripheral PbPb collisions at RHIC and LHC motivate a study in  $ep$  collisions. Two- and multi-particle correlations are studied in DIS, as well as photoproduction events with collision energy  $\langle W_{\gamma p} \rangle \sim 270$  GeV.

---

## Contents

<b>1 Introduction</b>	<b>2</b>
<b>2 Analysis Technique and Monte Carlo Generator</b>	<b>2</b>
<b>3 Results</b>	<b>3</b>
3.1 Charged-particle Multiplicity Spectra and Entanglement Entropy	3
3.2 Search for Collectivity in DIS and Photoproduction	4
<b>4 Conclusion</b>	<b>5</b>
<b>References</b>	<b>5</b>

---

## 1 Introduction

Quantum entanglement refers to the conjugate relationship on observables from two disconnected systems as they interact before. For deep inelastic scattering (DIS) in  $ep$  collision, quasi-free photon and remnant proton are naturally separate in the infinite-momentum frame, but have to form a colour-singlet state together due to confinement [1]. These two disconnected but correlated systems can provide an experimental test for the quantum entanglement on parton level with better-defined theoretical interpretations. The results can be an important reference for higher energy collisions [2].

Measurements in high multiplicity  $pA$  and  $pp$  collisions at RHIC and LHC [?, 3] have revealed similar collective behaviour to that in heavy-ion collisions. Yet it is unclear whether this collectivity observed in small systems also originates from hydrodynamic flow of a strongly interacting and expanding medium. Furthermore, the collision region of the  $pp$  and  $pA$  collisions is of the order of the proton size, while there is a smaller average size in  $ep$  collisions which depends on  $1/Q$ . In this sense, collectivity studies in positron-proton collisions at HERA H1 are expected to provide valuable information for the existence and origin of collective behaviour.

In this proceeding, we present quantum entanglement studies in  $ep$  DIS process, while the collective studies are carried out in both DIS and photoproduction processes. All DIS results in analyses are compared with theoretical predictions from Monte Carlo simulations including leading-order matrix elements, parton showers and hadronization.

## 2 Analysis Technique and Monte Carlo Generator

In DIS, as the probed and remnant region are entangled quantum mechanically, entanglement entropy of them should be identical. Based on these, the relation between entanglement entropy in DIS and gluon density can be simplified as  $S_{parton} = \ln[xG(x, Q^2)]$ , relating to parton distribution [1]. With "parton liberation" and "local parton-hadron duality (LPHD)" pictures, the relationship between initial-state parton entropy and final-state hadron entropy [4] can be expressed as:

$$S_{parton} = \ln[xG(x, Q^2)] = S_{hadron} = - \sum P(N) \ln P(N) \quad (1)$$

where  $P(N)$  is the charged particle multiplicity distribution which was measured in certain  $x_{bj}$  and  $Q^2$  regions. In this sense, the initial-state entropy as well as sub-nuclear information can be directly revealed by the final-state entropy through particle production, without considering fragmentation or other mechanism during space-time evolution.

On the other hand, an obvious signal of collectivity is the near-side, long-range ridge structure on two-particle azimuthal correlation function (2PC). The procedure to construct 2PC function is described in reference. The ridge yield can be extracted quantitatively through zero-yield-at-minimum (ZYAM) and bootstrap procedure. Based on 2PCs, anisotropies  $V_{n\Delta}$  can be possessed from Fourier coefficients from 1-D projections of 2PCs on  $\Delta\phi$  direction.

Comparing to 2PC, four-particle correlation function (4PC) [5] can better suppress short-range correlation. The H1 data is analysed with standard and subevent cumulant 4PC [6].

DIS process was simulated by Monte Carlo event generators (RAPGAP 3.1, DJANGO 1.4) within standard physics mechanism. The difference between RAPGAP 3.1 and DJANGO 1.4 [7] was their treatments on cascade which matched with first-order QCD calculations. There were DGLAP (Dokshitzer-Gribov-Lipatov-Altarelli-Parisi) evolution showers in the RAPGAP 3.1 [8], while the DJANGO 1.4 instead created dipoles between coloured partons within CDM (Colour Dipole Model). The generated events are passed through a detailed simulation of

the H1 detector response based on the GEANT3 simulation program and are processed using the same construction and analysis chain as used for data.

### 3 Results

The data in this analysis were collected using H1 detector at HERA from 2006 to 2007, with deep inelastic scattering (DIS) and photoproduction processes in positron-proton collisions at  $\sqrt{s} = 319$  GeV energy with an integrated luminosity  $136 \text{ pb}^{-1}$ .

Due to  $Q^2$  and scattered angle differing between two processes, different detectors are used for collecting final-state information. For DIS, online trigger requirements of cluster's radius and electromagnetic energy deposit on SpaCal are mentioned. Kinematic phase space is  $5 < Q^2 < 100 \text{ GeV}^2$ ,  $0.0375 < y < 0.6$ , and the  $y$  upper limit can also remove influence from photoproduction. In order to suppress QED initial state radiation and background events,  $z$  coordinate of vertex keeps in 35 cm around the nominal point, as well as triggered events satisfying  $35 < \sum_i (E_i - p_{z,i}) < 75 \text{ GeV}$ , where  $i$  loops for all hadronic final state (HFS) particles. For photoproduction, electron tagger instead records scattered electron signals with cooperation from photon detector. Collective studies requires selections on tagged energy and position. Besides, events must have at least one high- $p_T$  track ( $> 900 \text{ MeV}$ ) to ensure trigger efficiency.

For collectivity studies, multiplicity definitions are set on the number of tracks within  $0.3 < p_T^{lab} < 3.0 \text{ GeV}$  and  $-1.6 < \eta^{lab} < 1.6$ . Analyses in DIS and photoproduction processes use tracks with eta ranges of  $0 < \eta^{HCM} < 5$  and  $-1.6 < \eta^{lab} < 1.6$  respectively.

#### 3.1 Charged-particle Multiplicity Spectra and Entanglement Entropy

The charged-particle multiplicity distribution was measured in  $ep$  DIS at  $\sqrt{s} = 319$  GeV for particles with  $p_{T,lab} > 150 \text{ MeV}$  and  $|\eta_{lab}| < 1.6$  in laboratory frame [9]. According to the charged-particle distribution  $P(N)$  and Equation 1,  $S_{hadron}$  can be calculated to predict the  $S_{parton}$  of gluons at low- $x_{bj}$  region. Results shown in Figure 1 refer to moving  $\eta_{lab}$  window and current hemisphere with  $0 < \eta^* < 4$  respectively. These results indicate that our measurements disagree with the prediction from quantum entanglement.

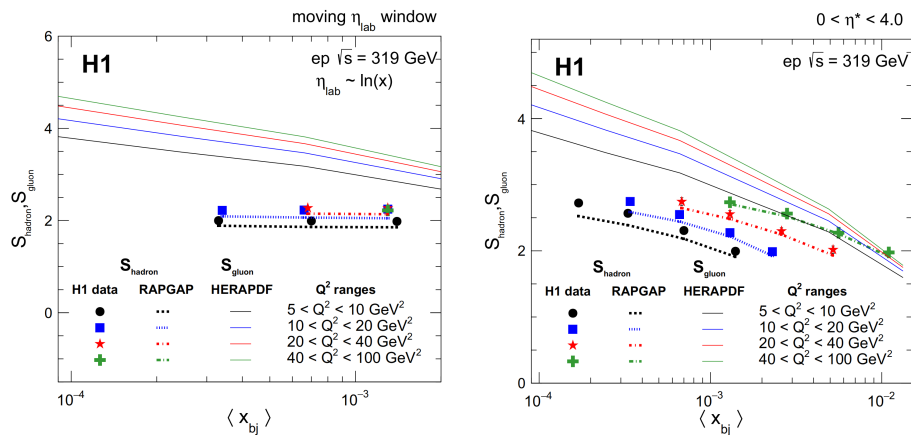


Figure 1:  $S_{hadron}$  calculated by charged-particle multiplicity distributions in  $ep$  DIS collisions at  $\sqrt{s} = 319$  GeV, compared with  $S_{parton}$  from gluon density. For left plot, as  $\eta_{lab} \sim \ln(x_{bj})$ , multiplicity definition changes as  $x_{bj}$  changes. For right plot, phase space is restricted by  $0 < \eta^* < 4$ .

### 3.2 Search for Collectivity in DIS and Photoproduction

The data used in our collective study is 13 million for DIS and 4.2 million for photoproduction. In the latter one, calculated centre-of-mass energy in  $\gamma p$  collisions is 270 GeV in average.

Figure 2 shows 2PCs in  $ep$  DIS collisions at  $\sqrt{s} = 319$  GeV, where there are no long-range, near-side ridge structure in both low and high multiplicity, indicating no sign of collective behaviours. Observing no that kind of structure, ridge yield limits are set by using a bootstrap process. Figure 3 shows  $1\sigma$  and  $2\sigma$  limits based on current statistics, which can be a good reference for future studies in small system. Figure 4 shows anisotropies  $V_{2\Delta}$ ,  $V_{3\Delta}$  extracted from 2PC's 1-D projections on  $\Delta\phi$  direction, in which the decreasing  $V_{2\Delta}$  trend and negative  $V_{3\Delta}$  indicate small room for the existence of ridge. Figure 5 shows 4PCs results with subevent cumulant methods. No negative  $C_2(4)$  also indicate no sign of collectivity.

Figure 4 and Figure 5 also show comparisons from RAPGAP and DJANGO simulation. RAPGAP has better description on data. As data can be described by Monte Carlo simulations without collectivity, there's small room for the existence of collectivity in data.

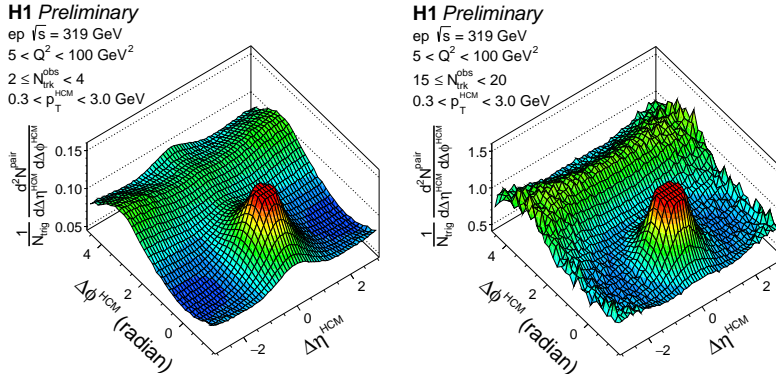


Figure 2: 2PCs in  $ep$  DIS collisions at  $\sqrt{s} = 319$  GeV, referring to  $2 \leq N_{trk}^{obs} < 4$  and  $15 \leq N_{trk}^{obs} < 20$  multiplicity regions from left to right.

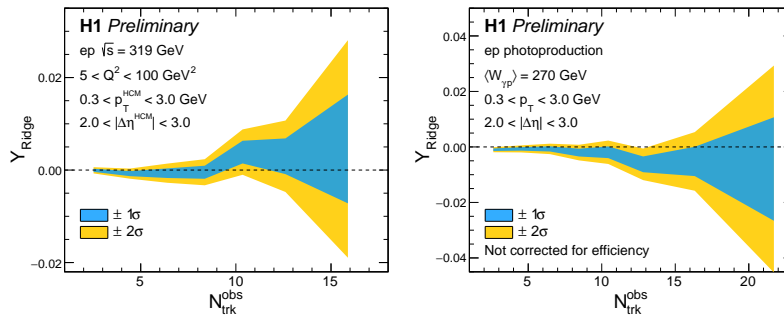


Figure 3: Ridge yield limits for  $1\sigma$  and  $2\sigma$  are set versus multiplicity in  $ep$  DIS process at  $\sqrt{s} = 319$  GeV and photoproduction process at  $\langle W_{\gamma p} \rangle \sim 270$  GeV from left to right, referring to  $2.0 < \Delta\eta < 3.0$  selections.

For 2PCs in  $ep$  photoproduction process at  $\langle W_{\gamma p} \rangle \sim 270$  GeV, there's neither near-side, long-range ridge structure nor collective behaviour signals from  $V_{2\Delta}$ ,  $V_{3\Delta}$  and  $C_2(4)$ . Similarly, observing no obvious ridge structure, ridge yield limits are set. Figure 6 show anisotropies  $V_{2\Delta}$ ,  $V_{3\Delta}$  extracted from 2PC's 1-D projections on  $\Delta\phi$  direction, which show similar trend as DIS results. Figure 7 shows 4PCs results with subevent cumulant methods, where no negative  $C_2(4)$  has been observed. Yet, solid conclusions in photoproduction process still wait for MC

simulation comparisons.

## 4 Conclusion

This is the first-time experimental test for quantum entanglement entropy. Although our measurements disagree with theoretical prediction. As for collective studies in  $ep$  collisions, there's no long-range, near-side ridge in either DIS or photoproduction 2PCs, so ridge yield limits are measured as reference for future higher luminosity  $ep$  collision experiments such as EIC. In DIS, anisotropies  $V_{2\Delta}$ ,  $V_{3\Delta}$  and  $C_2(4)$  can be described by RAPGAP simulations, indicating small room for the existence of collectivity. Also in photoproduction, anisotropies  $V_{2\Delta}$ ,  $V_{3\Delta}$  and  $C_2(4)$  indicate there is no collectivity.

## References

- [1] D. E. Kharzeev and E. M. Levin, *Deep inelastic scattering as a probe of entanglement*, Physical Review D **95**(11) (2017), doi:[10.1103/physrevd.95.114008](https://doi.org/10.1103/physrevd.95.114008).
- [2] Z. Tu, *Hera data on azimuthal decorrelation and charged particle multiplicity spectra probing qcd dynamics and quantum entanglement effects* (2020), [2011.02875](https://arxiv.org/abs/2011.02875).
- [3] A. M. Sirunyan, A. Tumasyan, W. Adam, F. Ambrogio, E. Asilar, T. Bergauer, J. Brandstetter, E. Brondolin, M. Dragicevic, J. Erö, M. Flechl, M. Friedl *et al.*, *Observation of correlated azimuthal anisotropy fourier harmonics in pp and p + Pb collisions at the lhc*, Phys. Rev. Lett. **120**, 092301 (2018), doi:[10.1103/PhysRevLett.120.092301](https://doi.org/10.1103/PhysRevLett.120.092301).
- [4] Z. Tu, D. E. Kharzeev and T. Ullrich, *Einstein-podolsky-rosen paradox and quantum entanglement at subnucleonic scales*, Physical Review Letters **124**(6) (2020), doi:[10.1103/physrevlett.124.062001](https://doi.org/10.1103/physrevlett.124.062001).
- [5] A. Bilandzic, R. Snellings and S. Voloshin, *Flow analysis with cumulants: Direct calculations*, Phys. Rev. C **83**, 044913 (2011), doi:[10.1103/PhysRevC.83.044913](https://doi.org/10.1103/PhysRevC.83.044913), [1010.0233](https://arxiv.org/abs/1010.0233).
- [6] J. Jia, M. Zhou and A. Trzupek, *Revealing long-range multiparticle collectivity in small collision systems via subevent cumulants*, Phys. Rev. C **96**(3), 034906 (2017), doi:[10.1103/PhysRevC.96.034906](https://doi.org/10.1103/PhysRevC.96.034906), [1701.03830](https://arxiv.org/abs/1701.03830).
- [7] K. Charchua, G. Schuler and H. Spiesberger, *Combined qed and qcd radiative effects in deep inelastic lepton-proton scattering: the monte carlo generator django6*, Computer Physics Communications **81**(3), 381 (1994), doi:[https://doi.org/10.1016/0010-4655\(94\)90086-8](https://doi.org/10.1016/0010-4655(94)90086-8).
- [8] H. Jung, *Hard diffractive scattering in high energy ep collisions and the monte carlo generator rapgap*, Computer Physics Communications **86**(1), 147 (1995), doi:[https://doi.org/10.1016/0010-4655\(94\)00150-Z](https://doi.org/10.1016/0010-4655(94)00150-Z).
- [9] V. Andreev *et al.*, *Measurement of charged particle multiplicity distributions in dis at hera and its implication to entanglement entropy of partons*, Eur. Phys. J. C **81**(3), 212 (2021), doi:[10.1140/epjc/s10052-021-08896-1](https://doi.org/10.1140/epjc/s10052-021-08896-1), [2011.01812](https://arxiv.org/abs/2011.01812).

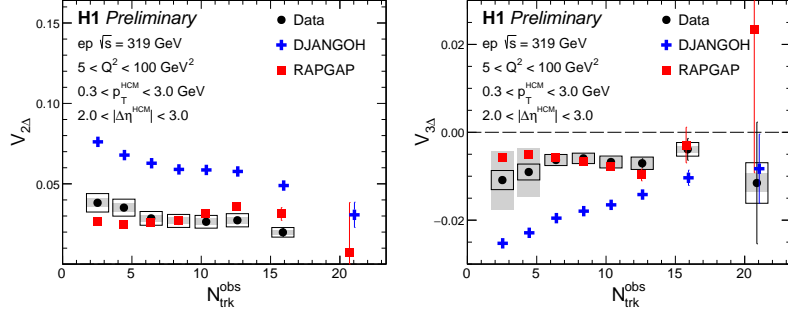


Figure 4: Anisotropies  $V_{2\Delta}$ ,  $V_{3\Delta}$  versus multiplicity extracted from  $ep$  DIS 2PCs' 1-D projections on  $\Delta\phi$  direction. Systematic uncertainties are shown as boxes (from MC simulation) and shadows (other sources).

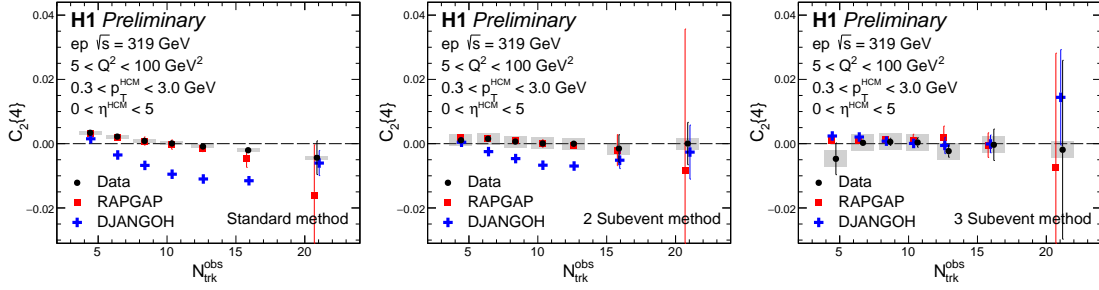


Figure 5:  $C_2(4)$  versus multiplicity in  $ep$  DIS at  $\sqrt{s} = 319$  GeV, within standard, 2-subevent and 3-subevent methods. This result is not corrected by efficiency.

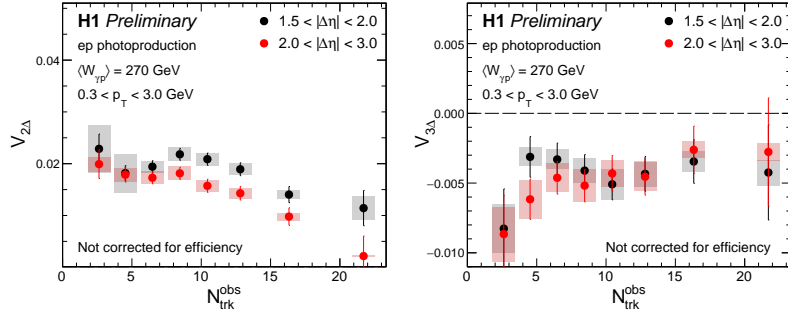


Figure 6: Anisotropies  $V_{2\Delta}$ ,  $V_{3\Delta}$  versus multiplicity extracted from  $ep$  photoproduction 2PCs' 1-D projections on  $\Delta\phi$  direction. Systematic uncertainties are shown as shadows.

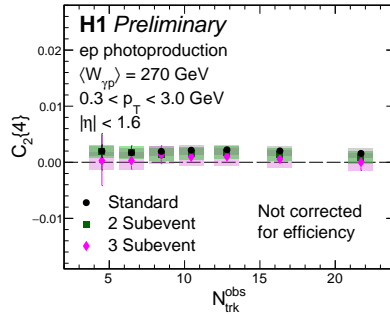


Figure 7:  $C_2(4)$  versus multiplicity in  $ep$  photoproduction process at  $\sqrt{s} = 319$  GeV, within standard, 2-subevent and 3-subevent methods.